Journal of The Electrochemical Society, **162** (1) B16-B21 (2015)
0013-4651/2015/162(1)/B16/6/$31.00 © The Electrochemical Society

An Organ-Like Titanium Carbide Material (MXene) with Multilayer Structure Encapsulating Hemoglobin for a Mediator-Free Biosensor

Fen Wang,[a] ChenHui Yang,[a,z] CongYue Duan,[b] Dan Xiao,[a] Yi Tang,[a] and JianFeng Zhu[a]

[a]*Key Laboratory of Auxiliary Chemistry & Technology for Chemical Industry, Ministry of Education, Shaanxi University of Science & Technology, Xi'an 710021, People's Republic of China*
[b]*School of Materials Science & Engineering, Shaanxi University of Science & Technology, Xi'an 710021, People's Republic of China*

A novel organ-like MXene-Ti_3C_2 nanomaterial was successfully prepared by etching Al from Ti_3AlC_2 in HF at room temperature and then used to immobilise hemoglobin (Hb) to fabricate a mediator-free biosensor with an oxidized surface. MXene-Ti_3C_2 and its morphology were well characterized by X-ray diffraction (XRD) and scanning electron microscopy (SEM), and the physical and electrochemical properties of as-obtained samples were studied by UV-vis diffuse reflectance spectra (DRS) and the electrochemical workstation. Spectroscopic and electrochemical results confirmed that MXene-Ti_3C_2 exhibited an excellent enzyme immobilization ability with biocompatibility for redox protein, displaying good protein bioactivity and stability. Due to the special structure and properties of MXene-Ti_3C_2, the direct electron transfer of Hb is facilitated and the prepared biosensors displayed good performance for the detection of H_2O_2 with a wide linear range of 0.1–260 μM for H_2O_2, as well as an extremely low detection limit of 20 nM (based on a signal-to-noise ratio of 3) for H_2O_2. The immobilization of proteins onto the surface of MXene-Ti_3C_2 is shown to be an efficient method for the development of a new class of sensitive, stable, and promising electrochemical biosensors.
 [DOI: 10.1149/2.0371501jes]

Manuscript submitted July 30, 2014; revised manuscript received September 15, 2014. Published November 8, 2014.

To accomplish the direct electron transfer (DET) between an enzyme and an electrode is of great importance in fabrication of mediator-free electrochemical biosensors.[1] Because the redox-active center of proteins is embedded in its protein shell deeply, DET between the protein and the electrode surface is generally difficult.[2–6] Moreover, the enzyme usually loses its bioactivity that adsorbed directly onto the electrode surface.[1,7] These problems make it difficult to transfer electrons directly at traditional electrodes.[1] Therefore, to employ nanomaterials is an efficient way to facilitate the direct electron transfer and retain the bioactivity of immobilized enzymes.[1,8–17] And among them, two-dimensional layered nanomaterials such as graphene[18–26] and MoS_2,[27–29] have attracted extensive attention to being used for immobilization of biomolecules onto electrode surface due to large specific surface areas, excellent electronic transport properties, and good biocompatibility.

However, as far as we know, the application of the novel graphene-like MXene-Ti_3C_2 nanomaterial, for constructing mediator-free biosensor has rarely been reported. In our study, MXene-Ti_3C_2 was successfully prepared by etching Al from Ti_3AlC_2 in HF at room temperature.[30–32] In general, Ti_3AlC_2 is a promising member of a large family of layered hexagonal (space group $P6_3/mmc$) ternary metal carbides and nitrides referred to as the $M_{n+1}AX_n$ phases, where "M" is an early transition metal, "A" is an A-group element (mostly groups 13 and 14), "X" is carbon or nitrogen, and n = 1, 2, 3, 4, 5 or 6.[33,34] This structure comprises Ti_6C octahedra, interleaved with layers of Al atoms. Immersing Ti_3AlC_2 phase in HF solution, results in the Al layers being selectively etched away. The Ti_3C_2 layers are terminated with mostly hydroxy group. With specific surface areas, MXene-Ti_3C_2 were found to be comparable to multilayer graphene.[30,35] The paralleled flake-like Ti_3C_2 layers could be less stable to reduce surface energy and tend to curve and become an organ-like structure for one end closing and the other end opening. Such organ-like structure should have a number of advantages as a support for enzyme immobilization. Just as schematic showes in Fig. 1, the organ-like structure is constructed with one end closing of the Ti_3C_2 nano-layers and the other end opening of that. Throughout the view of the organ-like structure, a large number of the Ti_3C_2 nano-layers with a large surface area point toward the closing end of the organ-like one, which is available for enzyme entrapment. The enzyme is adsorbed by surface functional groups of the nano-layers and funnelled toward the interior of the nano-layers that can become immobilized on the inner surfaces of the organ-like structure. They also could increase the resistance of the enzyme to leach during the reaction with the substrate. The substrate could have easy access to the immobilized enzyme in the interior of the organ-like structure, and in this narrow region, concentration of substrate and enzyme will enhance the chance of effective collisions between them. Therefore, the 2D organ-like multilayer structure should be a promising support for enzyme immobilization and have potential applications in biosensors.

In this paper, using hemoglobin (Hb) as a model protein, the constructed biosensor displayed a fast electron transfer of Hb and a good electrochemistry activity for the detection of H_2O_2 with wide linear range and low detection limit. Therefore, the present work offers a new avenue to broaden the applications of MXene in electrochemical biosensors.

Experimental

Preparation of materials.— The Ti_3AlC_2 powders were prepared by vacuum pressureless sintering method. Commercially available powders of TiC (particle size < 75 μm, 99.5% purity), Ti (particle size < 50 μm, 99.5% purity), Al (particle size < 75 μm, 99.5% purity) with a molar ratio of 2:1:1.2 were ball-milled for 1 h at a speed of 900 rpm. Afterward, the mixture was sintered at 1350 °C for 2 h in vacuum (less than 4.0×10^{-2} Pa). The sintered product was high-energy ball milled in absolute ethyl alcohol for 2 h, and then sifted out through a sieve (200 mesh) and dried at 50 °C for 24 hours.

The preparation of the MXene-Ti_3C_2 nanomaterial was organized as follows (Fig. S1–S3). Firstly, 2.0 g as-prepared Ti_3AlC_2 powders was immersed in 50 mL 40% HF solution under magnetic stirring at room temperature for 48 h. Then the resulting suspension was washed for 3 times by deionized water and 3 times by absolute ethanol, and centrifuged to separate the powders from the suspension. Finally, the powders dried in vacuum at 50 °C for 24 hours.

Hemoglobin (from bovine blood) and Nafion solution (5 wt% in lower aliphatic alcohols) were purchased from Sigma. All other chemicals (analytical grade without further purification) were purchased from Sinopharm Chemical Reagent Co., Ltd., China. In all experiments, deionized water was used.

Characterization.— The microstructure of the samples was investigated by field-emission scanning electron microscope (FE-SEM, JSM-6700, JEOL Ltd, Japan) on a Hitachi S-4800 & Hiroba EDX electron microscopy. The phase analysis of the samples was identified by X-ray diffraction (XRD, D/max-2200 PC X, Cu target, K_α radiation

[z]E-mail: ych488@163.com

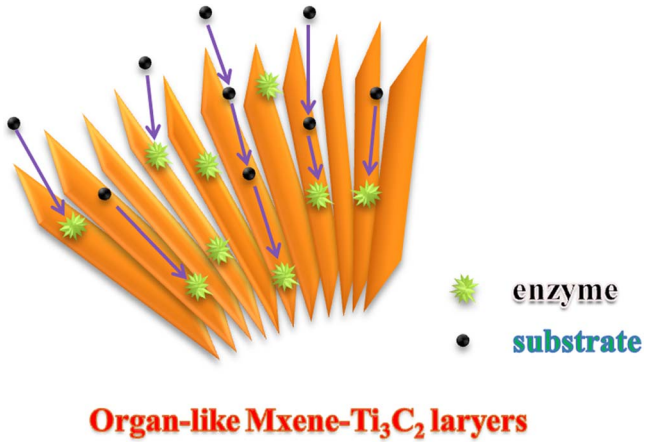

Figure 1. Schematic illustration of the organ-like structure of MXene-Ti_3C_2 nanomaterial encapsulating hemoglobin.

(40 KV and 30 mA)), a scanning step of 0.02 ° and scanning rate of 8 °/min were used. FT-IR spectra were obtained on a Bruker TENSOR27 instrument. All electrochemical experiments were performed with a CHI 660D electrochemical workstation (CH Instruments, Shanghai, China). A conventional three-electrode system was used for all electrochemical experiments, which consisted of a platinum wire as counter electrode, an Ag/AgCl/3M KCl as reference electrode, and a modified glassy carbon electrode (3 mm diameter) as working electrode. Unless otherwise noted, 0.1M pH 7.0 PBS was used as the electrolyte in all experiments. The buffer solution was purged with highly purified nitrogen for at least 30 min and a nitrogen atmosphere environment was kept in electrochemical measurements.

Electrochemical testing.— To investigate the electrochemical behavior of MXene-Ti_3C_2 in the H_2O_2 biosensor, enzyme electrode was assembled. Prior to use, a glassy carbon (GC) electrode was polished with 0.3 and 0.05 μm alumina slurry, and sonicated in ethanol and water successively. The cleaned GC electrode was dried using a purified nitrogen stream. The enzyme electrode was prepared by a simple casting method. Firstly, 1 mL of 2 mg mL^{-1} MXene-Ti_3C_2 suspension and 0.5 mL of 10 mg mL^{-1} Hb PBS were mixed and stirred for 30 min. Next, 0.5 mL of Nafion (5%) was added to the mixture and then stirred for 10 min. Finally, 4 μL of the mixture was applied to the surface of a freshly polished GC electrode to prepare the Nafion/Hb/Ti_3C_2/GC electrode and then stored in refrigerator prior to use. In order to comparison, Nafion/Ti_3C_2/GC electrode was also constructed as above procedure except Hb. Before electrochemical measurements, all the as-prepared film electrodes were immersed in pH 7.0 PBS for 30 min to remove residual components.

Results and Discussion

Characterization of MXene-Ti_3C_2.— Fig. 2(a) shows SEM image of Ti_3AlC_2 after HF treatment confirms successful exfoliation of individual particles, which is similar to what was reported for exfoliated graphite[21,22] or Ti_3AlC_2,[30] where the layers are clearly separated from each other compared to the unreacted powders (Figure S1). Fig. 2(b) shows the partial enlarged SEM image of the Ti_3C_2 layers. In Fig. 2, the Ti_3C_2 layers are less than 20 nm in average, which indicates that the Ti_3C_2 layers have the large specific surface areas. Hb could be adsorbed on the large surfaces of the Ti_3C_2 layers which provide a protective microenvironment for the Hb to retain their activity (Figure S3). Hence, the MXene-Ti_3C_2 nanomaterial with multilayer structure is accessible for Hb to be immobilized.

Fig. 3 shows XRD pattern of Ti_3AlC_2 after HF treatment, and the diffraction pattern was analyzed for $Ti_3C_2(OH)_2$ by using MID Jade5. And the diffraction peaks is in good agreement between the simulated XRD spectra for $Ti_3C_2(OH)_2$.[30] The Ti_3C_2 layers should present suitable surface for ligand interaction, on account of possessing two exposed Ti atoms per unit formula. Since the experiments were conducted in an aqueous environment rich, hydroxyl is the most probable ligand. And the experimental results provides strong evidence of the formation of $Ti_3C_2(OH)_2$.

Spectroscopic characterization of Nafion/Hb/Ti_3C_2 composite film.— FTIR spectroscopy is an effective means to explore the secondary structure of Hb entrapped in the composite film.[6,26,36] The shapes of amide I and amide II bands of protein provide detailed information on the secondary structure of polypeptide chain.[37] As shown by the FTIR spectrum of Hb (curve a) in Fig. 4, the amide I band (1700–1600 cm^{-1}) results from C=O stretching vibration of peptide linkages in the backbone of protein. The amide II band (1620–1500 cm^{-1}) is caused by the combination of N–H bending and C–N stretching. As shown in Fig. 4, the spectrum of amide I and II bands of Hb in Nafion/Hb/Ti_3C_2 composite film (curve b) (1659 and 1541 cm^{-1}) are almost the same as that obtained for native Hb (1658 and 1539 cm^{-1}), and are essentially consistent with the reported value of native Hb.[6,26,36,38] The similarity of the two spectra demonstrates that Hb retained the essential features of its native secondary structure in the Nafion/Ti_3C_2 composite film. This MXene-Ti_3C_2 with good biocompatibility shows a promising matrix for protein immobilization and biosensor fabrication.

Direct electrochemistry of Hb on Nafion/Ti_3C_2 films.— Fig. 5 displays the typical cyclic voltammograms (CVs) of different modified electrodes in 0.1 M PBS (pH 7.0) at a scan rate of 0.1V s^{-1}. No redox peak is observed at Nafion/Ti_3C_2/GC electrode (curve a), which indicates that Nafion/Ti_3C_2/GC electrode is electroinactive in the potential window. The Nafion/Hb/Ti_3C_2/GC electrode (curve b) exhibits a

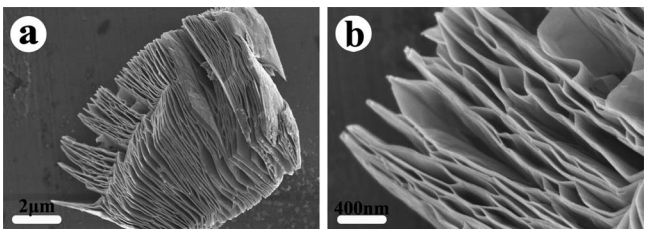

Figure 2. SEM images of (a) MXene-Ti_3C_2 and (b) the high-magnification of (a).

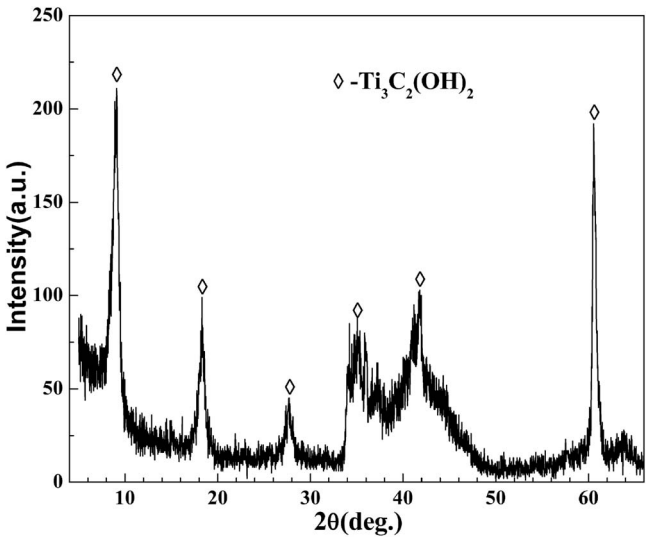

Figure 3. XRD pattern of Ti_3AlC_2 after HF treatment, and the diffraction pattern was analyzed for $Ti_3C_2(OH)_2$ by using MID Jade5.

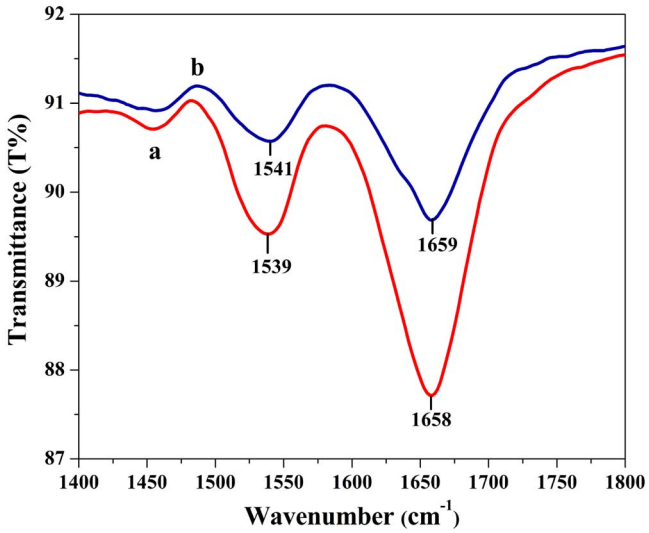

Figure 4. UV–Vis absorption spectra of (a)Hb, (b) Hb-Ti_3C_2.

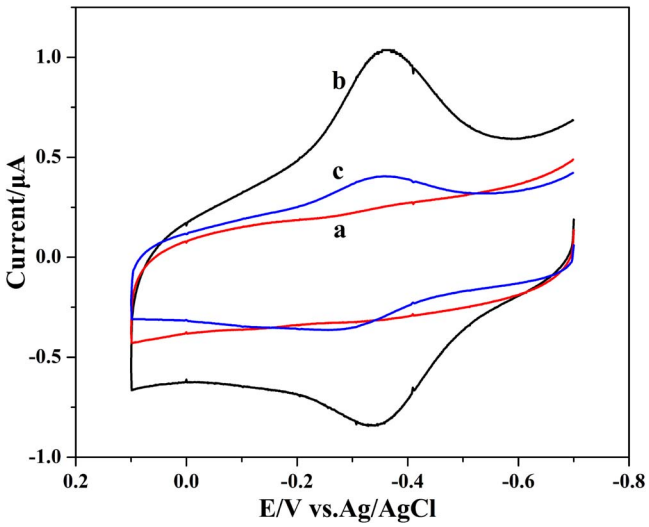

Figure 5. Cyclic voltammograms of the Nafion/Ti_3C_2/GC electrode (a), Nafion/Hb/Ti_3C_2/GC electrode (b), Nafion/Hb/GC electrode (c) in 0.1M pH 7.0 PBS with a scan rate of 0.1 V s^{-1}.

couple of stable and well-defined redox peaks at −0.367 V and −0.327 V vs. Ag/AgCl, which could be ascribed to direct electron transfer between Hb and the underlying electrode. According to Lu et al.,[6] the electron transfer of Hb occurs between the Fe^{III} and Fe^{II} site within Hb. The formal potential ($E^{0'} = (E_{p,a}+E_{p,c})/2$) of Hb was −0.347 V vs. Ag/AgCl is in agreement with −0.345 V vs. Ag/AgCl reported for the Hb($Fe^{III/II}$) redox couple in Hb-ZnO-Nafion.[6] The potential difference (ΔE_p) between the anodic and cathodic peak potential is about 40 mV. Such a small ΔE_p value reveals a fast and quasi-reversible electron-transfer process, revealing that MXene-Ti_3C_2 can provide a favorable microenvironment for Hb to undergo a facile electron-transfer reaction. Compared with that of Nafion/Hb/Ti_3C_2/GC electrode, the redox peaks observed at Nafion/Hb/GC electrode (curve c, in Fig. 5) are 79.7% smaller, suggesting an enhanced electron transfer between Hb molecules and the surface of Nafion/Hb/Ti_3C_2/GC electrode. Meanwhile, the much smaller redox peaks of Nafion/Hb/GC electrode can be attributed to the deep burying electroactive center of the protein structure and the denaturation of proteins on the bare electrode surface, and it is difficult for proteins to realize the DET process on the bare electrode.[39] It can be clearly seen from the comparison that direct electron transfer between Hb molecules and GC electrode is greatly enhanced at Nafion/Hb/Ti_3C_2/GC electrode.

Fig. 6(A) shows the cyclic voltammograms of 0.1 M PBS (pH 7.0) at a Nafion/Hb/Ti_3C_2/GC electrode when the scan rate was increased from 0.1 to 0.8 V s^{-1}. With the increase of the scan rates, the cathodic and anodic peak currents of Hb increase simultaneously, while the cathodic and anodic peak potentials show a small shift and the peak to peak separation also become slightly enlarged. Fig. 6(B) shows that the cathodic (I_{pc}) and anodic (I_{pa}) peak currents increase linearly with scan rates from 0.1 to 0.8 V s^{-1} (linear regression equations: $I_{pc}(\mu A) = 0.00302$ v (mV s^{-1}) + 0.0790, $R^2 = 0.999$; $I_{ac}(\mu A) = 0.00308$ v (mV s^{-1}) + 0.0483, $R^2 = 0.998$). This reveals that the electrode reaction corresponds to a surface-controlled quasi-reversible process. Using the Laviron method for a surface-controlled electrochemical system,[40] the apparent heterogeneous electron transfer rate constant (k_s) of Hb immobilized on Nafion/Hb/Ti_3C_2/GC electrode is estimated to be about 3.6 s^{-1}, which is higher than the value reported for Hb immobilized porous nanosheet-based ZnO microspheres (3.2 s^{-1}),[6] and TiO_2 nanorods-graphene (0.65 s^{-1}),[36] suggesting a faster electron-transfer process. This means that MXene-Ti_3C_2 facilitates the direct electron transfer of Hb.

Fig. 7 shows the cyclic voltammograms of 0.1 M PBS of different pH at a Nafion/Hb/Ti_3C_2/GC electrode. Stable and well-defined CVs were observed in the pH range 6.0∼8.0. With the increase of pH value, both the cathodic and anodic peaks shifted to the negative

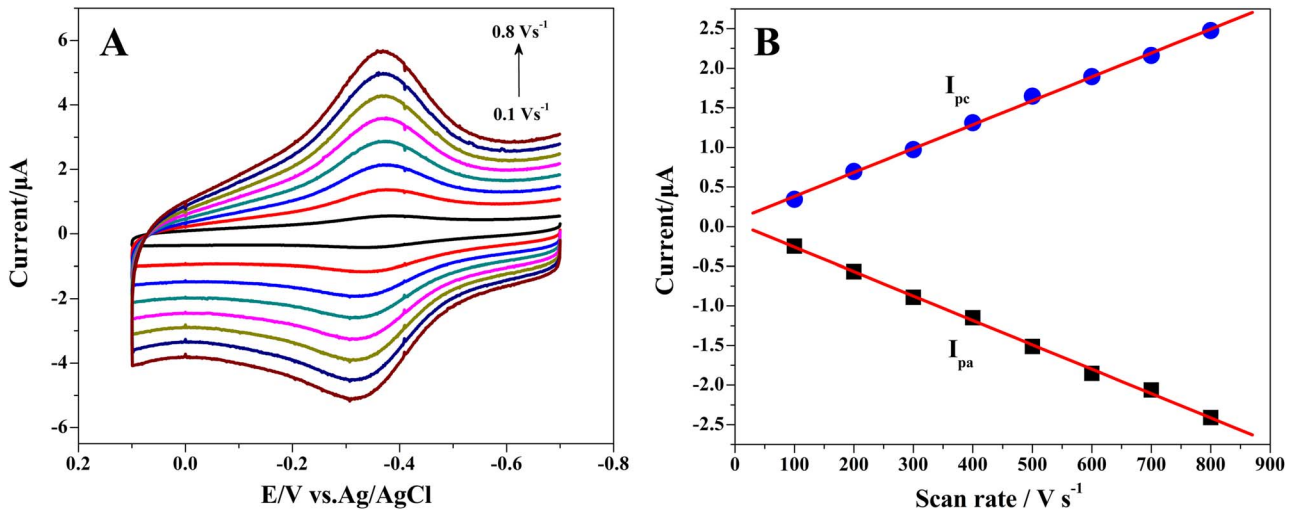

Figure 6. (A) Cyclic voltammograms of the Nafion/Hb/Ti_3C_2/GC electrode in 0.1 M pH 7.0 PBS with increasing scan rates from 0.1 to 0.8 Vs^{-1}. (B) The cathodic and anodic peak current vs. scan rate.

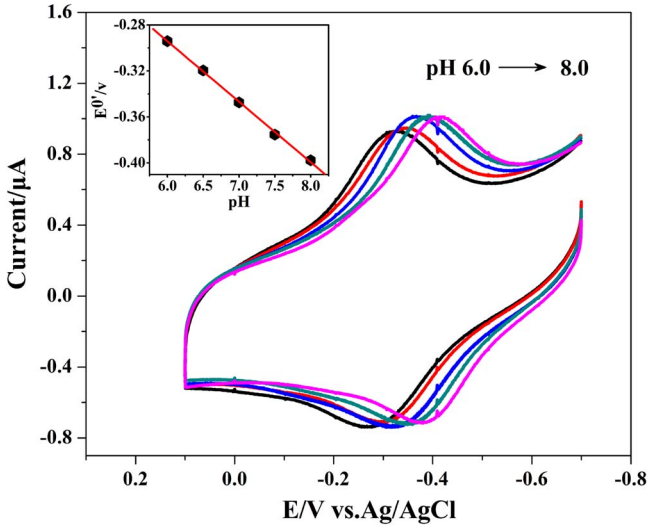

Figure 7. Cyclic voltammograms of the Nafion/Hb/Ti_3C_2/GC electrode in 0.1 M PBS with different pH values: 6.0 (a), 6.5 (b), 7.0 (c), 7.5 (d) and 8.0 (e). Inset: plot of formal potential vs. pH value.

(Fig. 7). This can be contributed to the involvement of proton transfer in the $Hb(Fe^{III})/Hb(Fe^{II})$ redox couple.[26,36] The $E^{0\prime}$ value of Hb varied linearly in the range of pH 6.0∼8.0, with a slop of −52.4 mV pH^{-1} (the inset of Fig. 7). This value is very close to the theoretical value for the transfer of one proton and electron in a reversible reduction (−58mV pH^{-1} at 25°C).[26,36,41,42]

Electrocatalytic properties of the Nafion/Hb/Ti_3C_2/GC electrode.— When Hb is immobilized on an electrode surface with retained bioactivity, it usually exhibits electrocatalytic activity for H_2O_2, nitrite and Cl_3CCOOH.[1,6,26,36] By using H_2O_2 as a probe, the electrocatalytic properties of the Nafion/Hb/Ti_3C_2/GC electrode were investigated. As shown in Fig. 8, the reduction peak increased dramatically with the addition of H_2O_2, accompanied by a decrease and disappearance of the oxidation peak, displaying the obvious electrocatalytic behavior of Hb for the reduction of H_2O_2.[6,26] A possible reaction mechanism of H_2O_2 catalyzed by the Hb-based

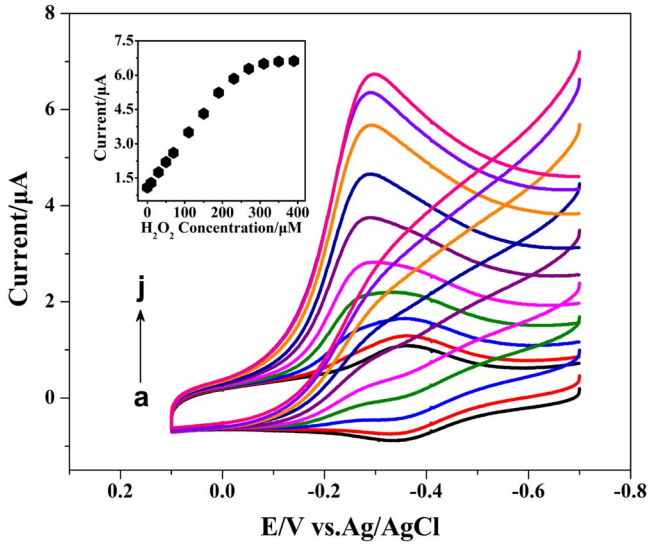

Figure 8. Cyclic voltammograms of the Nafion/Hb/Ti_3C_2/GC electrode in 0.1 M pH 7.0 PBS containing 0 (a), 10 (b), 30 (c), 50 (d), 70 (e), 110 (f), 150 (g), 190 (h), 230 (i), 310 (j) H_2O_2 with a scan rate of 0.1 V s^{-1}.

electrode is postulated as follows:[43]

$$Hb(Fe^{III}) + e^- \rightleftharpoons Hb(Fe^{II})$$

$$Hb(Fe^{II}) + H_2O_2 + 2H^+ \rightarrow Hb(Fe^{III}) + 2H_2O$$

On increasing the H_2O_2 concentration, the current value reached a saturation limit (the inset of Fig. 8), and saturation behavior was characteristic of enzyme-based catalysis. The apparent Michaelis-Menten constant (K_M^{app}) can be obtained by the electrochemical-version of Lineweaver-Burk equation:[44]

$$\frac{1}{I_{ss}} = \frac{K_M^{app}}{I_{max}C} + \frac{1}{I_{max}}$$

where I_{ss} is the steady-state current after the addition of substrate, C is the bulk concentration of the substrate, and I_{max} is the maximum current measured under saturated substrate conditions. The K_M^{app} value for Nafion/Hb/Ti_3C_2/GC electrode was estimated to be 95 μM. This value was smaller than those ever reported values of 3300 μM,[36] and 928 μM,[45] indicating that Hb immobilized on Nafion/Hb/Ti_3C_2/GC electrode retained higher bioactivity.

Biosensor performance of the Nafion/Hb/Ti_3C_2/GC electrode.— The biosensor performance for the detection of H_2O_2 of the Nafion/Hb/Ti_3C_2/GC electrode was also investigated by amperometry. Fig. 9(A) gives the amperometric responses of Nafion/Hb/Ti_3C_2/GC electrode at −0.35 V after adding H_2O_2 in stirred PBS (pH 7.0). Fig. 9(A) demonstrates the response time (achieving 95% of the steady-state current) was less than 3 s. Moreover, a well-defined linear relationship between the current and the H_2O_2 concentration was observed. The calibration plot (Fig. 9(B)) showed a linear range from 0.1 to 260 μM with a correlation coefficient of 0.9988 (N = 39). The detection limit was estimated to be 0.02 μM (based on a signal-to-noise ratio of 3). Performances of various H_2O_2 biosensors are listed in Table I. It is clear that the performance of Nafion/Hb/Ti_3C_2/GC electrode was significantly improved. There are some reasons why the Nafion/Hb/Ti_3C_2/GC electrode displays both a lower detection limit and a wider linear range. Firstly, MXene-Ti_3C_2 nano-layers provide a favorable microenvironment for the protein to retain its activity and stability. More importantly, the substrate can simply be entrapped by MXene-Ti_3C_2 with high surface areas and the special organ-like structure, and have easy access to the enzymes immobilized on the surface of MXene-Ti_3C_2 nano-layers. There is an increased chance of effective collisions between substrate and redox protein leading to improved performance of this sensor.[41]

Reproducibility and stability of the biosensor.— The long-term stability of fabricated biosensors was studied by examining its current response after storage at 4°C. The biosensors could retain 93% of the initial response after 3 weeks storage, demonstrating good long-term stability. The good long-term stability can be contributed to the good biocompatibility of the MXene-Ti_3C_2 nano-layers with multilayer structure, which can provide a favorable microenvironment for Hb to retain its bioactivity.

The reproducibility of the biosensor was investigated by determining 4 μM H_2O_2 in PBS (pH 7.0). The relative standard deviation (R.S.D) was 2.1% respectively for 5 successive measurements. Five biosensors prepared under the same conditions independently gave a R.S.D. of 2.6% for the determination of 4 μM, indicating an acceptable electrode-to-electrode reproducibility.

Conclusions

The 2D organ-like MXene-Ti_3C_2 nanomaterial was successfully prepared by etching Al from Ti_3AlC_2 in HF. The organ-like nano-layers were subsequently used to fabricate mediator-free biosensors for the detection of H_2O_2. The biosensors exhibited a low detection limit of 20 nM and a liner range of 0.1–260 μM for H_2O_2. The improved performance of the biosensor can be attributed to the unique morphology and property of MXene-Ti_3C_2. Firstly, the MXene-Ti_3C_2

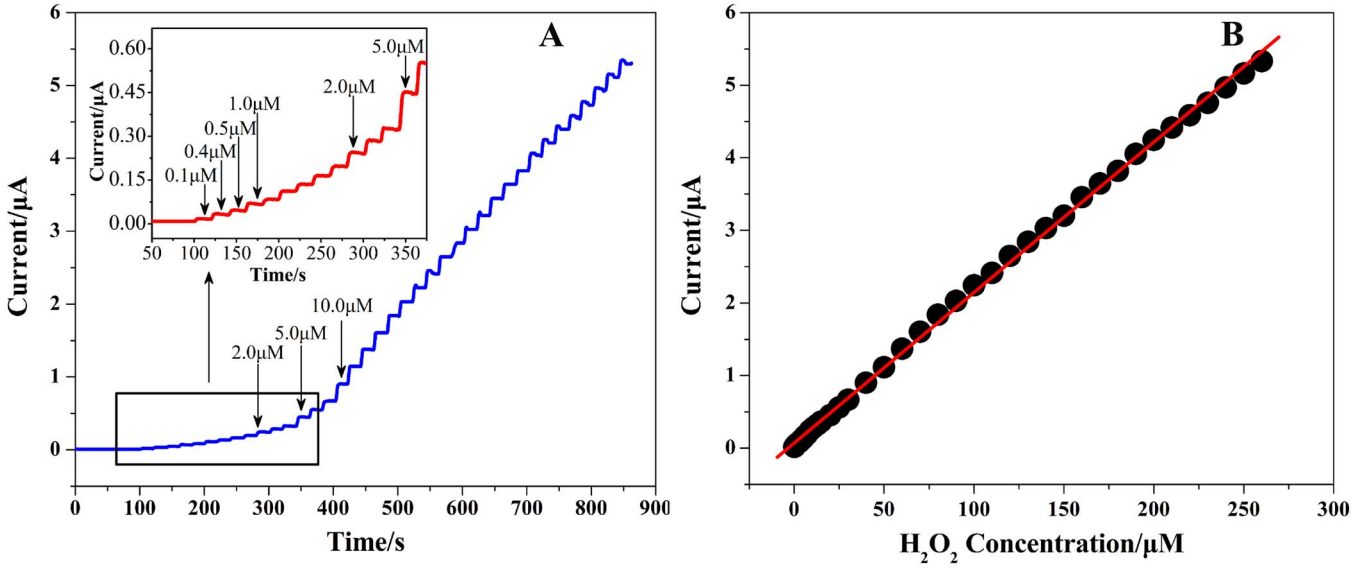

Figure 9. (A) Typical current-time response of the Nafion/Hb/Ti_3C_2/GC electrode at -0.35 V to successive addition of H_2O_2 in stirred 0.1 M pH 7.0 PBS. (B) The stready state current vs. H_2O_2 concentration.

Table I. Comparison of the performances of the various electrochemical biosensors for H_2O_2.

Modified electrodes	Linear range/(μM)	Detection limit (μM)	Stability (percentage/days)	Reference
Nafion/Hb/Ti_3C_2/GCE	0.1–260	0.02	93%/21	This work
Hb/CMC-TiO_2-NTs/GCE	4–64	0.63	90%/21	17
Hb/TiO_2NS-rGO/Nafion/GCE	0.1–145	0.01	93.6%/21	26
Hb/ZnO-MWCNTs/Nafion/GCE	1–80	0.85	93%/30	38
HRP/TiO_2 microspheres with hollow core-shell structure/Nafion/GCE	0.4–140	0.05	94%/21	41
PVA/Hb/MWCNTs/CILE	1.2–30.0	1.00	95.3%/14	42
PDDA-G/GCE	9.42–139.42	10	89.5%/35	46
PB-nitrobenzene-RGO/GCE	1.2–15250	0.4	–	47

CMC is Carboxymethyl cellulose, as one of the hydrogel; TiO_2NS-rGO, titania nanosheet modified reduced graphene oxide; MWCNT, multi-walled carbon nanotube; PDDA, poly(diallyldimethylammoniumchloride); PB-nitrobenzene-RGO/GCE, Prussian blue (PB) nanocubes-nitrobenzene-reduced graphene oxide (RGO) nanocomposites.

nano-layers provide a favorable microenvironment for the protein to retain its activity and stability. More importantly, the substrate can simply be entrapped by MXene-Ti_3C_2 with high surface areas and the special organ-like structure, and have easy access to the enzymes immobilized on the surface of the MXene-Ti_3C_2 nano-layers. There is an increased chance of effective collisions between substrate and redox protein leading to improved performance of this sensor. MXene-Ti_3C_2 was demonstrated to be a promising matrix for the fabrication of mediator-free biosensors, and may find wide potential applications in environmental analysis and biomedical detection.

Acknowledgments

This work was supported by the National Natural Science Foundation of China (51472153, 51171096), and the Graduate Innovation Fund of Shaanxi University of Science and Technology.

References

1. Y. Wang, X. L. Ma, Y. Wen, Y. Y. Xing, Z. R. Zhang, and H. F. Yang, *Biosens. Bioelectron.*, **25**, 2442 (2010).
2. F. A. Armstrong , H. A. O. Hill and N. J. Walton, *Acc. Chem. Res.*, **21**, 407 (1988).
3. A. Heller, *Accounts Chem. Res.*, **23**, 128 (1990).
4. F. W. Scheller, N. Bistolas, S. Q. Liu, M. Janchen, M. Katterle, and U. Wollenberger, *Adv. Colloid Interface Sci.*, **116**, 111 (2005).
5. X. B. Lu, J. Q. Hu, X. Yao, Z. P. Wang, and J. H. Li, *Biomacromolecules*, **7**, 975 (2006).
6. X. B. Lu, H. J. Zhang, Y. W. Ni, Q. Zhang, and J. P. Chen, *Biosens. Bioelectron.*,**24**, 93 (2008).
7. J. Hong, H. Ghourchian, and A. A. Moosavi–Movahedi, *Electrochem. Commun.*, **8**, 1572 (2006).
8. G. F. Fu , P. S. Vary and C.-T. Lin, *J. Phys. Chem. B*, **109**, 8889 (2005).
9. M. Jin, X. T. Zhang, S. Nishimoto, Z. Y. Liu, D. A. Tryk, A. V. Emeline, T. Murakami, and A. Fujishima, *J. Phys. Chem. C*, **111**, 658 (2007).
10. B. H. Liu, Y. Cao, D. D. Chen, J. L. Kong, and J. Q. Deng, *Anal. Chim. Acta*, **478**, 59 (2003).
11. L. P. Ma, R. Yuan, Y. Q. Chai, and S. H. Chen, *J. Mol. Catal. B: Enzyme*, **56**, 215 (2009).
12. J. D. Qiu, H. P. Peng, R. P. Liang, and X. H. Xia, *Biosens. Bioelectron.*, **25**, 1447 (2010).
13. W. Sun, Z. Q. Zhai, D. D. Wang, S. F. Liu, and K. Jiao, *Bioelectrochemistry*, **74**, 295 (2009).
14. J. W. Wang, L. P. Wang, J. W. Di, and Y. F. Tu, *Talanta*, **77**, 1454 (2009).
15. G. Yang, R. Yuan, and Y. Q. Chai, *Colloid. Surf. B*, **61**, 93 (2008).
16. B. D. Yao, Y. F. Chan, X. Y. Zhang, W. F. Zhang, Z. Y. Yang, and N. Wang, *Appl. Phys. Lett.*, **82**, 281 (2003).
17. W. Zheng, Y. F. Zheng, K. W. Jin, and N. Wang, *Talanta*, **74**, 1414 (2008).
18. R. Shrivastavaa, R. Sharma, S. P. Satsangeea, and R. Jainb, *J. Electrochem. Soc.*, **159**, B795 (2012).
19. M. Y. Elahi, A. A. Khodadadi, and Y. Mortazavi, *J. Electrochem. Soc.*, **161**, B81 (2014).
20. R. Jain, R. Sharma, R. K. Yadav, and R. Shrivastava, *J. Electrochem. Soc.*, **160**, H179 (2013).
21. G. X. Wang, J. Yang, J. Park, X. L. Gou, B. Wang, H. Liu, and J. Yao, *J. Phys. Chem. C*, **112**, 8192 (2008).
22. G. X. Wang, X. Shen, B. Wang, J. Yao, and J. Park, *Carbon*, **47**, 1359 (2009).
23. X. L. Li, X. R. Wang, L. Zhang, S. W. Lee, and H. J. Dai, *Science*, **319**, 1229 (2008).
24. X. H. Zhu, Q. F. Jiao, X. X. Zuo, X. Xiao, Y. Liang, and J. M. Nan, *J. Electrochem. Soc.*, **160**, H699 (2013).
25. C. X. Feng, G. Q. Xu, H. P. Liu, J. Lv, Z. X. Zheng, and Y. C. Wu, *J. Electrochem. Soc.*, **161**, B1 (2014).
26. H. Liu, C. Y. Duan, X. Su, X. N. Dong, Z. Huang, W. Q. Shen, and Z. F. Zhu, *Sensor Actuat. B-Chem.*, **203**, 303 (2014).

27. J. Xiao, D. Choi, L. Cosimbescu, P. Koech, J. Liu, and J. P. Lemmon, *Chem. Mater.*, **22**, 4522 (2010).
28. J. Xiao, X. J. Wang, X. Q. Yang, S. D. Xun, G. Liu, P. K. Koech, J. Liu, and J. P. Lemmon, *Adv. Funct. Mater.*, **21**, 2840 (2011).
29. C. F. Zhang, H. B. Wu, Z. P. Guo, and X. W. Lou, *Electrochem. Commun.*, **20**, 7 (2012).
30. M. Naguib, M. Kurtoglu, V. Presser, J. Lu, J. J. Niu, M. Heon, L. Hultman, Y. Gogotsi, and M. W. Barsoum, *Adv. Mater.*, **23**, 4248 (2011).
31. X. H. Wang and Y. C. Zhou, *J. Mater. Sci. Technol.*, **26**, 385 (2010).
32. N. V. Tzenov and M. W. Barsoum, *J. Am. Ceram. Soc.*, **83**, 825 (2000).
33. M. W. Barsoum, *Prog. Solid State Chem.*, **28**, 201 (2000).
34. C. F Hu, H. B. Zhang, F. Z. Li, Q. Huang, and Y. W. Bao, *Int. J. Refract. Met. H. Mater.*, **36**, 300 (2013).
35. M. Naguib, O. Mashtalir, J. Carle, V. Presser, J. Lu, L. Hultman, Y. Gogotsi, and M. W. Barsoum, *ACS Nano*, **6**, 1322 (2012).
36. W. Sun, Y. Q. Guo, X. M. Ju, Y. Y. Zhang, X. Z. Wang, and Z. F. Sun, *Biosens. Bioelectron.*, **42**, 207 (2013).
37. J. K. Kauppinen, D. J. Moffate, H. H. Mantsch, and D. G. Lameron, *Appl. Spectrosc.*, **35**, 271 (1981).
38. W. Ma and D. B. Tian, *Bioelectrochemistry*, **78**, 106 (2010).
39. X. B. Lu, J. H. Zhou, W. Lu, Q. Liu, and J. H. Li, *Biosens. Bioelectron.*, **23**, 1236 (2008).
40. E. Laviron, *J. Electroanal. Chem.*, **101**, 19 (1979).
41. Q. Xie, Y. Y. Zhao, X. Chen, H. M Liu, D. G. Evans, and W. S. Yang, *Biomaterials*, **32**, 6588 (2011).
42. F. H. Wu, J. J. Xu, Y. Tian, Z. C. Hu, L. W. Wang, and Y. Z. Xian, *Biosens. Bioelectron.*, **24**, 198 (2008).
43. E. E. Ferapontova, *Electroanal.*, **16**, 1101 (2004).
44. R. A. Kamin and G.S. Wilson, *Anal. Chem.*, **52**, 1198 (1980).
45. W. Sun, X. Q. Li, Y. Wang, R. J. Zhao, and K. Jiao, *Electrochim. Acta*, **54**, 4141 (2009).
46. L. P. Jia, J. F. Liu, and H. S. Wang, *Electrochim. Acta*, **111**, 411 (2013).
47. L. Wang, Y. J. Yea, X. P. Lua, Y. Wua, L. L. Sun, H. L. Tan, F. G. Xu, and Y. H. Song, *Electrochim. Acta*, **114**, 223 (2013).